Numerical modeling of induced seismicity associated with fluid injection and withdrawal using 2D discrete element fracture network model

J.S. Yoon[1] & A. Zang[1] & G. Zimmermann[2,3] & O. Stephansson[1]
GFZ German Research Centre for Geosciences, Potsdam, Germany
[1]*Section 2.6, Seismic Hazard and Stress Field*
[2]*Section 4.1, Reservoir Technologies*
[3]*International Centre for Geothermal Research ICGR*

ABSTRACT: This study investigates induced seismicity in deep geothermal reservoir associated with fluid injection and production in doublet and triplet reservoir systems with a hydro-mechanical coupled numerical model. The model is using 2D discrete element model with embedded discrete fracture network. Fluid injection is performed for 6 hours with sequentially increased flow rate in three steps and the resulting induced seismicity is monitored. It is followed by constant rate fluid production at a point (doublet) and at two points (triplet) distances away from the injection point maintained for 20 hours. Spatio-temporal distribution of fluid pressure, injection/production induced seismic events, their magnitudes and source characters are investigated. The simulation shows that production induced seismic events mostly occur along the line at steep fluid pressure gradient with mostly implosion source characteristics. It was simulated that larger magnitude events can be induced in the vicinity of the production well and near pre-existing fractures when combined with abrupt slipping.

1 INTRODUCTION

Hydraulic stimulation is essential in developing Enhanced Geothermal Systems (EGS) to increase reservoir permeability and maximize heat energy extraction. Byproduct of hydraulic stimulation is induced microseismic events that can trigger some events with higher magnitudes.

As well as fluid injection, production of fluid can also induce seismic events resulting from pore pressure decline and large contraction of the reservoir, in particular increasing horizontal stresses above and below the reservoir that could lead to reverse faulting (Segall 1989). The Lacq gas field in sourth western France offers one of the best-documented cases of seismicity induced by extraction of pore fluids (Grasso and Wittlinger 1990, Segall et al. 1994).

Seismicity induced by fluid withdrawal cannot be explained without taking into account the accompanying stress changes, which are associated with the larger-scale contraction of the reservoir caused by pore pressure reduction. The magnitude of the events can be potentially large.

With this background, this numerical modelling study aims at investigating the following issues: (1) Can fluid production generate major earthquakes in the vicinity of the production well? (2) Can fluid production result in the seismic activity further away from the production well? (3) What are the source characteristics of the fluid production induced seismic events? (4) Where do they occur? (5) Can fluid production induce larger magnitude events in the already stimulated reservoir?

2 RESERVOIR MODEL

Figure 1 shows the constructed reservoir model which is represented by circular disk discrete elements bonded at their contacting points with prespecified strength that can bear tensile and shear strength following Mohr-Coulomb failure criterion. Fluid flow algorithm is additionally implemented where the white empty space surrounded by disks is treated as pore space in geological porous media and referred to here as 'virtual pore'. Virtual pores which can store some fluid pressure are all interconnected and flow between pores occurs through the connecting flow channel governed by cubic law which is a function of hydraulic aperture (e), pressure difference (ΔP), flow channel length (L), and fluid dynamic viscosity (μ). Fluid pressure built up at the virtual pore exerts forces on the surrounding disks, which consequently changes the stress state at the disk contacts. Mode I tensile crack occurs when the tensile stress exceeds the predefined tensile strength at the disk contact. Mode II shear crack occurs when the shear stress exceeds the Mohr-Coulomb failure envelope. Upon crack occurrence, the accumulated strain energy is released as a stress

drop and seismic wave is propagated to the surrounding. Seismicity computation algorithm enables capturing the radiated seismic wave and constructs a moment tensor for each crack occurring in porous rock matrix (Hazzard and Young 2002, 2004). Yoon et al. (2013) modified the algorithm so as to compute resulting magnitude and radiated seismic energy of an induced event resulting from Mode I and Mode II failure of pre-existing joints represented by smooth joint contact model.

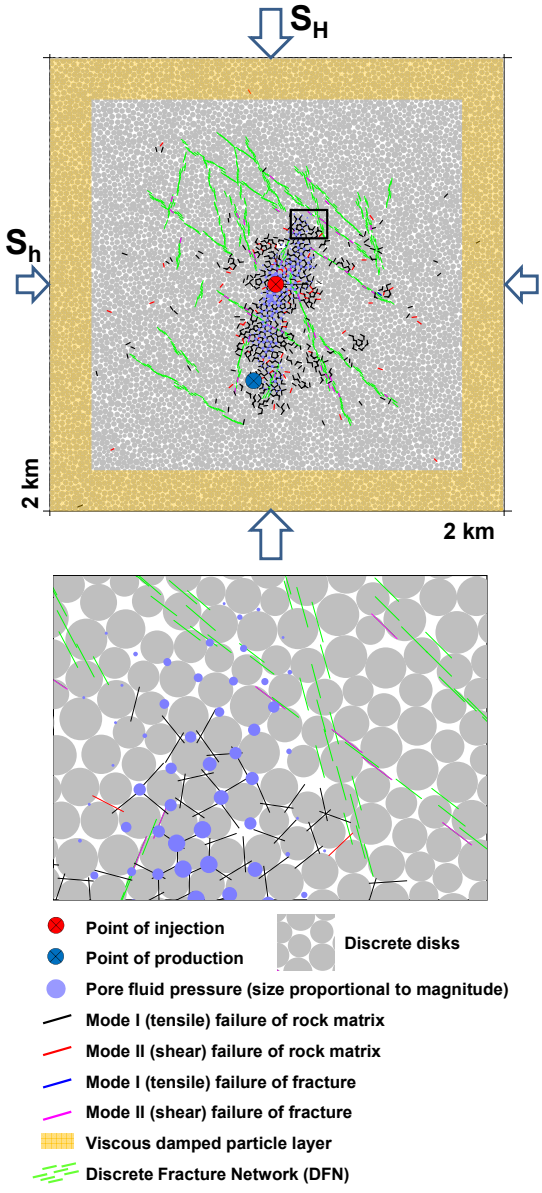

Figure 1. (a) Reservoir model (stimulated) in 2 km x 2 km size with embedded fracture network and subjected to anisotropic in-situ stress of S_H = 75 MPa and S_h = 60 MPa; (b) Close-up view of boxed area showing concept of hydro-mechanical coupling scheme: discrete particles (gray), void spaces filled with inter-connected pores.

3 SIMULATION OF DOUBLET SYSTEM

For a doublet reservoir system, one well at model centre (x=0, y=0) is used for massive fluid injection for stimulation of reservoir, creating induced seismicity and enhancing permeability and the other well (x=-100, y=-450, SSW of injection point) is used for fluid production.

Figure 2 shows applied flow rate for injection (sequential step-wise: 10, 12.5, 15 liter per second maintained for 2 hours each) and production (5 liter per second maintained for 20 hours) and moment magnitudes (Mw) of the induced events versus time. Events with moment magnitudes larger than 1 (over the red dashed line) are marked by red stars.

Figure 3 shows spatio-temporal distribution of fluid injection and production induced seismic events. Colour represents their time of occurrence. In general, the shape of the induced seismic event cloud is elliptic, extending longer in NS. Slight deviation from NS is due to presence of pre-existing discrete fracture network. Induced events associated with fluid production (occurrence time > 40 hr.) are marked by green to blue, which are located at bottom tip of the induced event cloud.

Occurrence of induced seismic events are further classified into four stages in Figure 4, (a) during injection (Time = 0-6.5 hr.), (b) after shut-in (Time = 6.5-38 hr.), (c) during production (Time = 38-58 hr.), (d) after production (Time = 58-80 hr.).

Figure 5 shows contour plots of fluid pressure distribution evolving with time. Distribution of fluid pressure during injection and after shut-in (a-c) matches well with the spatial distribution of induced seismic events. Fluid production commences at 38 hr. and fluid pressure around the production well decreases and size of the fluid free area grows.

Boundary between fluid free zone and high fluid pressure zone (where the fluid pressure gradient is steep, i.e. Figure 5f, 5g) well matches with the location of induced seismic events shown in Figure 4d.

Each induced seismic event has moment magnitude which is computed from the moment tensor algorithm (Hazzard et al. 2002, 2004; Yoon et al. 2013). By analysing the moment tensor components of each induced event and decomposing it in isotropic and deviatoric parts (Jost and Hermann 1989), R values are computed using the following equation:

$$R = \frac{tr(M) * 100}{\left(|tr(M)| + \sum |mi *|\right)} \quad (1)$$

where, $tr(M)$ is the trace of the moment tensor, $tr(M)=m_1+m_2$, representing the volume change at the source, $mi*$ are the deviatoric eigenvalues. The R varies from 66% (pure explosion) to -66% (pure implosion), and R = 0 indicates a pure shear failure mechanism (Feiniger and Young 1992). An event is assumed to have a significant isotropic component if the R > 30%, implosional if R < -30%.

Figure 6 shows the histograms of the R values of the induced seismic event that occurred in doublet system, (a) during injection, (b) after shut-in, (c) during production, (d) after production. Fluid injec-

tion results in relatively large number of positive and negative volume changing source (Figure 6a). After shut-in, there appear more events with implosion characters, but also with explosion and shear characters. However, during and after production majority of the induced events are implosion sources.

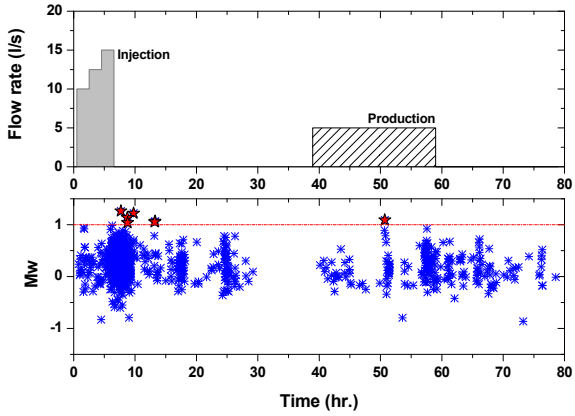

Figure 2. Sequential step-wise fluid injection (Time = 0-6.5 hr.) followed by fluid withdrawal (Time = 38-58 hr.) in doublet system. Moment magnitudes of induced seismic events versus time. Red stars are events with Mw>1 (above the red dashed line).

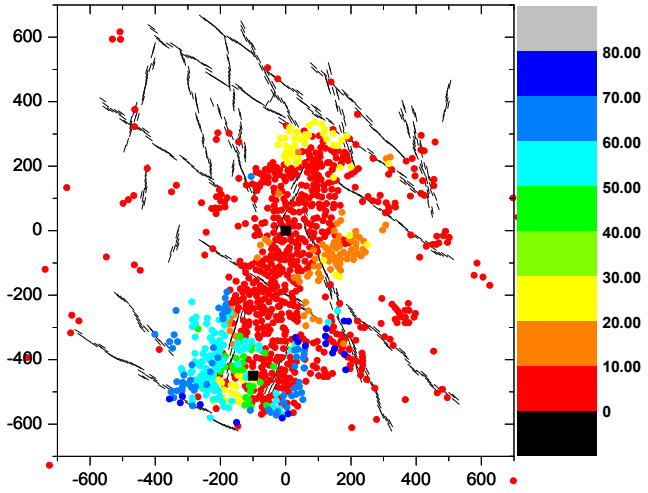

Figure 3. Spatio-temporal distribution of induced seismic events from fluid injection and withdrawal in doublet system. Colour codes according to time of occurrence in unit of hour.

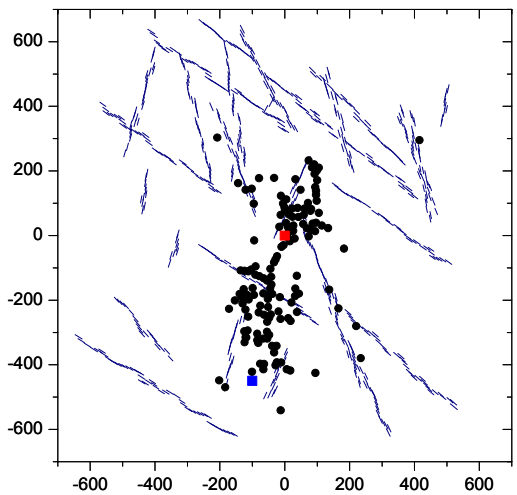

(a) pre-shut-in (Time = 0-6.5 hr.)

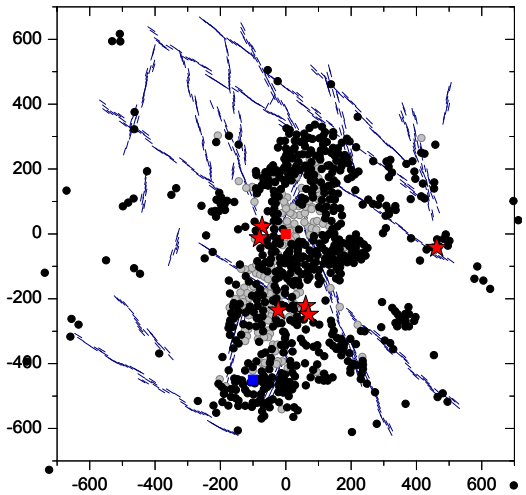

(b) post-shut-in (Time = 6.5-30 hr.)

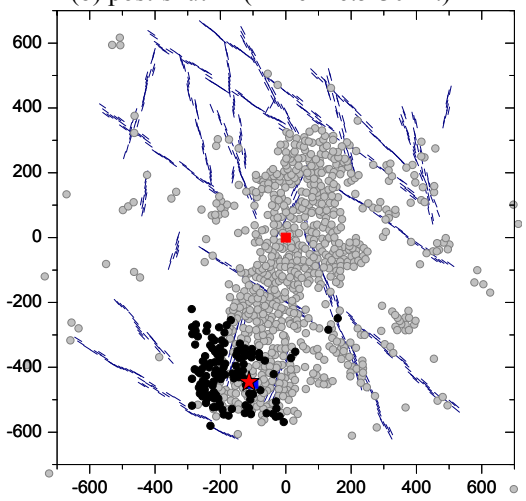

(c) during production (Time = 38-58 hr.)

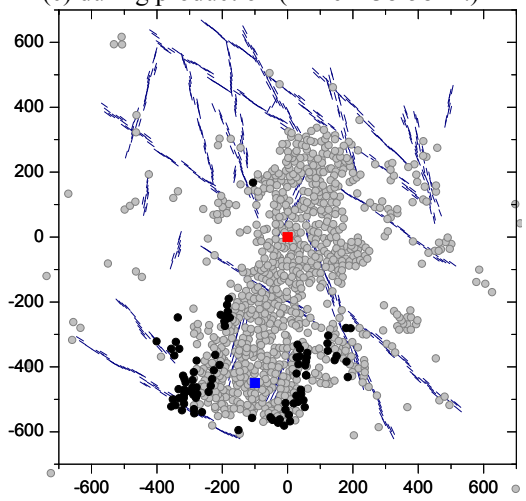

(d) after production (Time = 58-80 hr.)

Figure 4. Distribution of induced seismic events occurred (a) during fluid injection (Time = 0-6.5 hr.), (b) after shut-in (Time = 6.5-30 hr.), (c) during fluid production (Time = 38-58 hr.), (d) after production (Time = 58-80 hr.) in doublet system. Red and blue squares are fluid injection and production points, respectively.

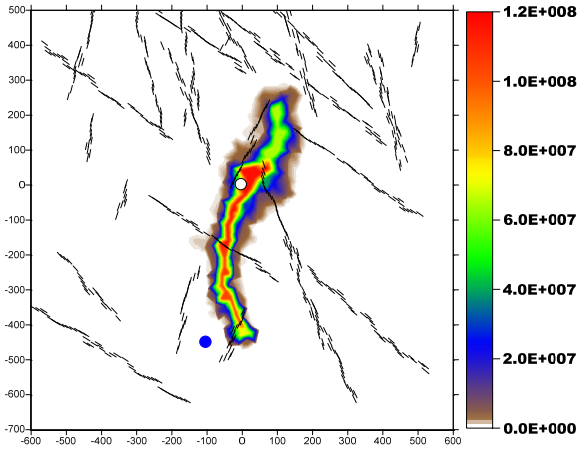

(a) Time = 6.5 hr.

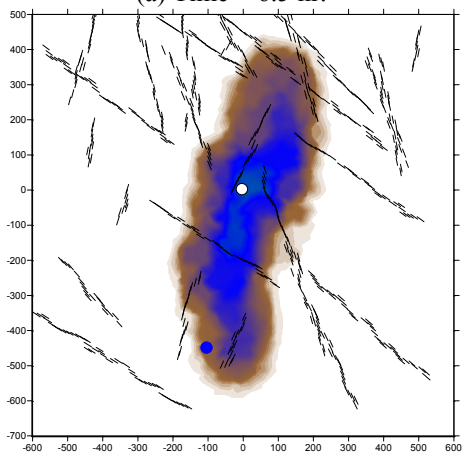

(b) Time = 30 hr.

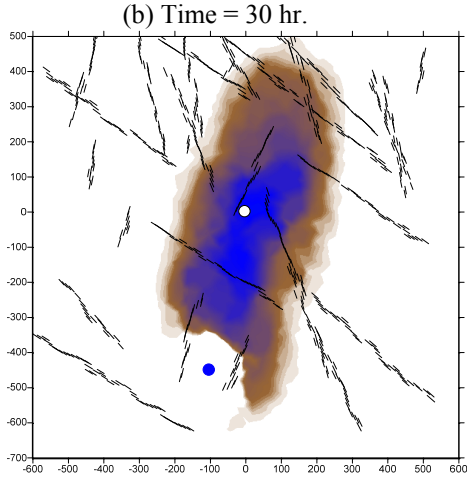

(c) Time = 60 hr.

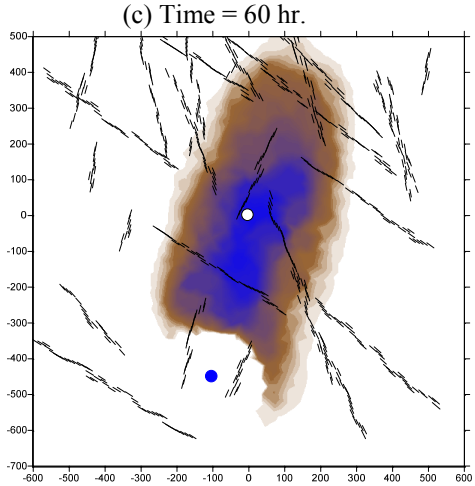

(d) Time = 80 hr.

Figure 5. Distribution of fluid pressure in doublet system at time, (a) 6.5 hr., (b) 3 hr., (c) 60 hr., (d) 80 hr. Colour scale in (a) represents fluid pressure in unit of Pascal (Pa). White and blue dots are fluid injection and production points, respectively.

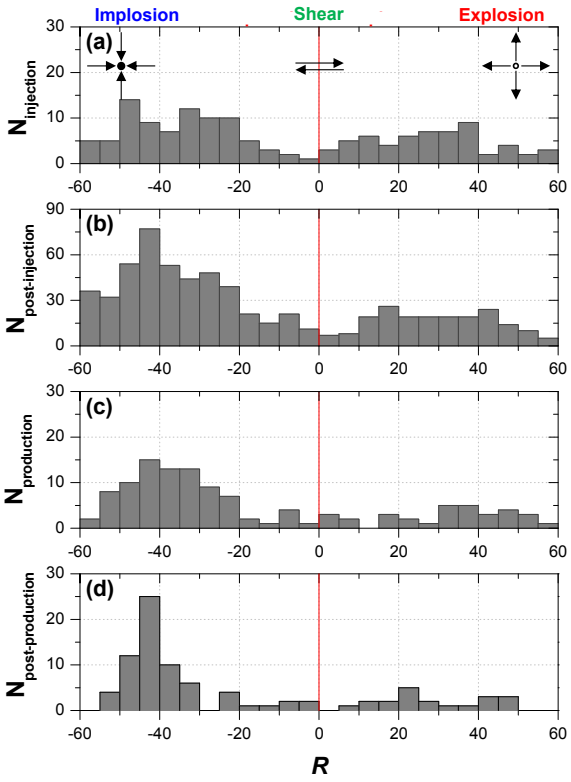

Figure 6. Histogram of the R values of the induced seismic events occurred in doublet system, (a) during fluid injection, (b) after shut-in, (c) during production, (d) after production.

Figure 7 shows location of induced seismic events occurred (a) during production and (b) after production and their *R* values. During production, there occur many events in the vicinity of the production point with mixed portion of explosion and implosion sources. After production, events are more implosional sources and occur along the outer-rim of the event cloud generated during production.

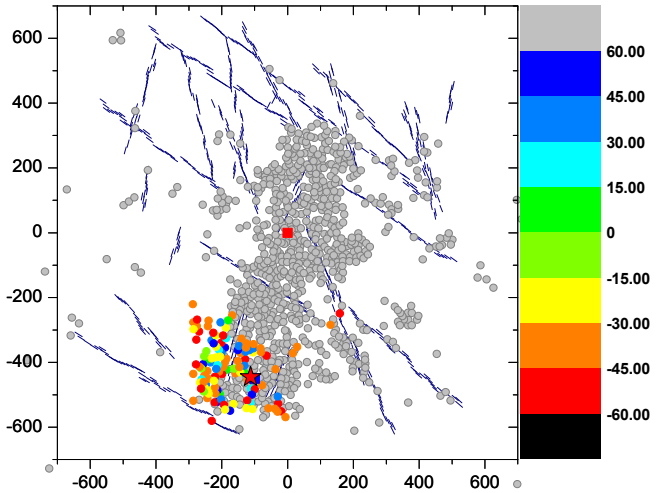

(a) during production (Time = 38-58 hr.)

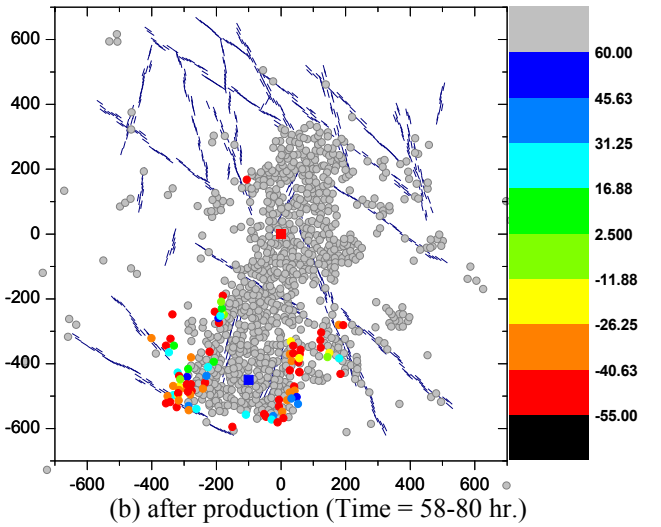

(b) after production (Time = 58-80 hr.)

Figure 7. Distribution of induced seismic events occurred (a) during production and (b) after production and their R values in doublet system.

4 TRIPLET SYSTEM

This section deals with triplet reservoir system where one well at the model centre (x=0, y=0) is used for massive fluid injection for stimulation of reservoir and two wells (#1: x=-100, y=-450; #2: x=100, y=300, SSW and NNE of the injection points, respectively) are used to fluid production.

Figure 8 shows applied flow rate for injection (sequential step-wise: 10, 12.5, 15 liter per second maintained for 2 hours each) and fluid production at two wells, where 5 and 8 liter per second rate is applied to well #1 and #2 and both maintained for 20 hours and moment magnitudes (Mw) of the induced events versus time. Events with moment magnitudes larger than 1 (over the red dashed line) are marked by red stars.

Figure 9 shows spatio-temporal distribution of induced events of which time of occurrence is represented by the colour scale. Similar to the previous doublet reservoir system, induced events associated with fluid production (occurrence time > 40 hr.) are marked by green to blue, which are located at top and bottom tips of the induced event cloud. Figure 10 displays the histograms of the *R* values of the induced seismic events occurred (a) during production and (b) after production. The histogram shows that the most of the induced events are implosional sources. Figure 11 shows location of induced seismic events occurred (a) during production and (b) after production and their *R* values. Similar to the doublet system, induced seismic events at the rim are mostly implosion sources, partially mixed with shear (green) and explosional (light blue to blue) sources.

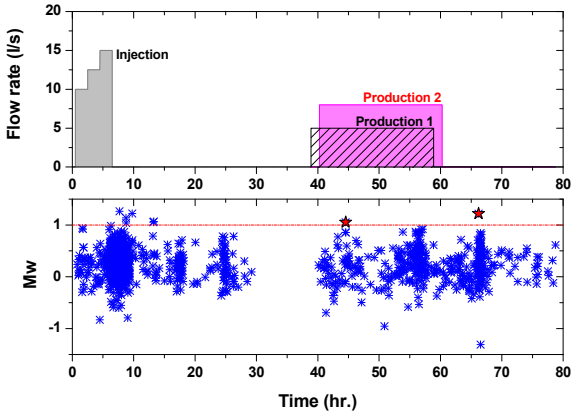

Figure 8. Sequential step-wise fluid injection (Time = 0-6.5 hr.) followed by fluid production (Time = 38-60 hr.) in triplet system and moment magnitudes of induced seismic events versus time. Red stars are events with Mw>1 (above the red dashed line).

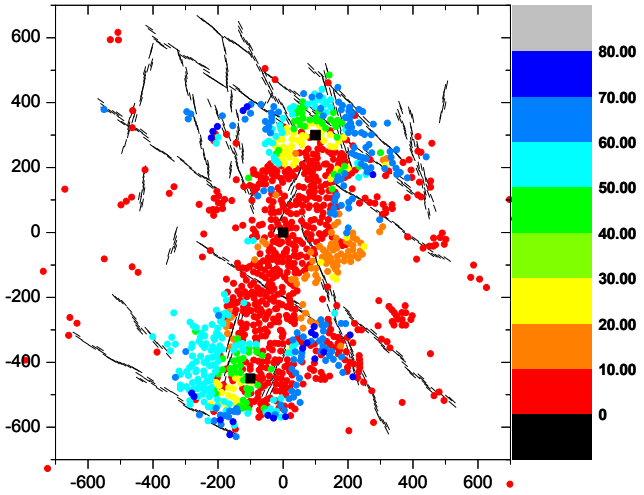

Figure 9. Spatio-temporal distribution of induced seismic events from fluid injection and withdrawal in triplet system. Colour codes according to time of occurrence in unit of hour

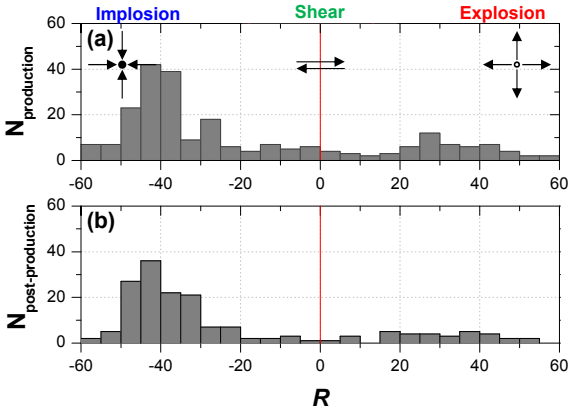

Figure 10. Histogram of the R values of the induced seismic events occurred in triplet system, (a) during production (Time = 38-60 hr.), (b) after production (Time = 60-80 hr.).

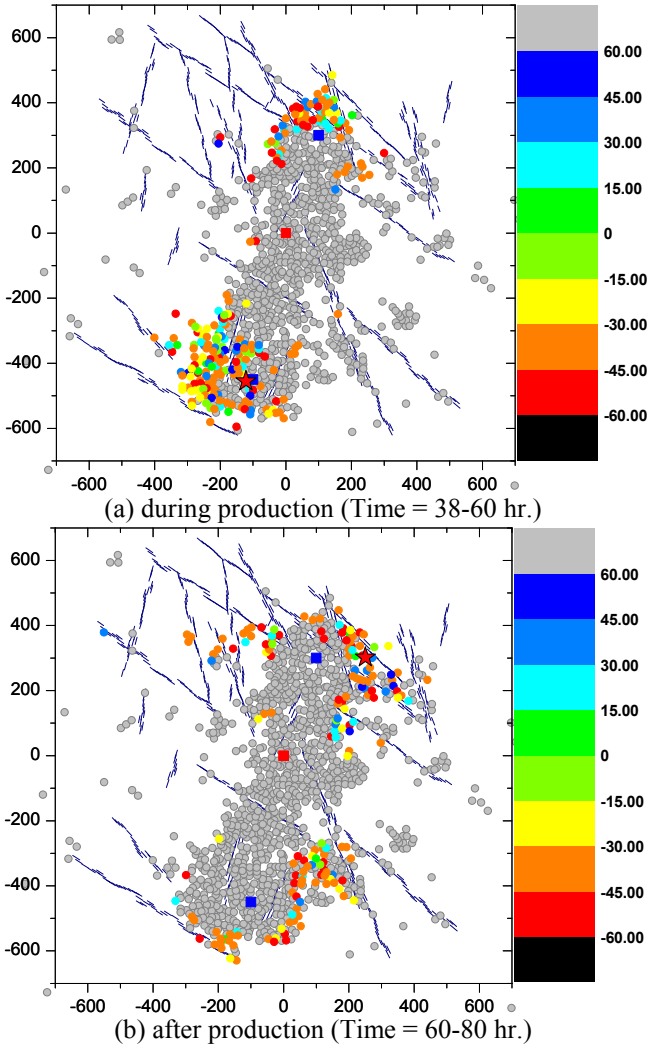

Figure 11. Distribution of induced seismic events occurred (a) during production and (b) after production and their R values in triplet system.

5 SUMMARY AND CONCLUSIONS

This study deals with simulation of fluid injection and production and associated induced seismicity in fractured crystalline reservoir subjected to anisotropic in-situ stress. Stress changes due to fluid injection and production result in failure of rock matrix and pre-existing fractures in Mode I (tensile) and Mode II (shear) from which seismicity characters (magnitude and source mechanisms) are computed. Fluid injection and production are simulated in doublet system (one injection well, one production well) and triplet reservoir system (one injection well, two production wells) and the following conclusions are made.

1) Fluid production can generate induced events with relatively larger magnitudes in the vicinity of the production well.
2) There can be a few seismic events induced at some distance away from the production well.
3) During production, densely clustered events with mixed portion of implosion and explosion characteristics occur in the vicinity of the production point in dense cluster with larger magnitude events.
4) After production, additional events occurred along the outer rim of the event cloud generated during production. Source characters are more implosional.
5) In both doublet and triplet reservoir systems, it is shown that fluid production can result in additional induced seismic events with a few larger magnitude events occurring in the vicinity of the production well and near pre-existing fractures when combined with abrupt slipping.

6 ACKNOWLEDGEMENT

This work was financially supported by the German Federal Ministry for the Environment, Nature Conservation and Nuclear Safety under grant 0325451C. We thank Dr. Jim Hazzard from Itasca for the fluid flow algorithm and allowing modification and use for this study. Review and comments from Dr. Oliver Heidbach (GFZ) are appreciated.

REFERENCES

Feignier, B. & Young, R.P. 1992. Moment tensor inversion of induced microseismic events: Evidence of non-shear-failures in the -4<M<-2 moment magnitude range. *Geophysical Research Letters* 19(14): 1503-1506.

Grasso, J.R. & Wittlinger, G. 1990. Ten years of seismic monitoring over a gas field area. *Bulletin of the Seismological Society of America* 80(2): 450-473.

Hazzard, J.F. & Young, R.P. 2002. Moment tensors and micromechanical model. *Tectonophysics* 356: 181-197.

Hazzard, J.F. & Young, R.P. 2004. Dynamic modelling of induced seismicity. *International Journal of Rock Mechanics & Mining Sciences* 41: 1365-1376.

Jost, M.L. & Herrmann, R.B. 1989. A student's guide to and review of moment tensors. *Seismological Research Letters* 60: 37-57.

Segall, P. 1989. Earthquakes triggered by fluid extraction. *Geology* 17: 942-946.

Segall, P., Grasso, J.R. & Mossop, A. 1994. Poroelastic stressing and induced seismicity near the Lacq gas field, southwestern France. *Journal of Geophysical Research* 99(B8): 15423-15438.

Yoon, J.S., Zang, A. & Stephansson, O. 2013. Kaiser stress observation and simulation in deep geothermal reservoirs using hydro-mechanical coupled discrete element fracture network model. Submitted to *Geothermics* Special Issue "Induced Seismicity".